Published in final edited form as:

*Neutron News*. 2015 ; 26(2): . doi:10.1080/10448632.2015.1028273.

# Applications of neutron imaging and future possibilities

**Daniel S. Hussey**,

**David L. Jacobson**

Physical Measurement Laboratory, National Institute of Standards and Technology, 100 Bureau Dr., MS 8461, Gaithersburg, MD 20899, USA

## Introduction

Neutron imaging applications exploit the power of neutrons to penetrate through metals and measure small concentrations of hydrogen and lithium with high sensitivity. Recent advances in digital imaging devices have enabled many novel neutron imaging experiments and methods. This article highlights recent experiments that demonstrate the expanding range of neutron imaging. All of these applications would benefit from higher resolution (time, spatial, neutron energy) and we speculate on the ability of new methods to meet these needs.

## Electrochemical Energy Storage and Conversion

Electrochemical energy sources share many common features, a hydrogenous electrolyte, metallic or graphitic electrodes, light mobile ions such as hydrogen or lithium, and a metallic casing; a perfect situation for neutron imaging.

### Proton Exchange Membrane Fuel Cells (PEMFCs)

There has been a sustained effort to understand water transport phenomena in PEMFCs [1]. Sufficient membrane hydration is required for efficient high power production operation, but water entrained elsewhere impedes reactant flow and can result in degradation. An important development for PEMFC research was neutron imaging detector spatial resolution improved from about 250 μm to 25 μm in 2006 and then to 13 μm in 2009 [2]. This enabled researchers to study the through-plane water distribution in the GDLs and in thick membranes or electrodes. As an example, Los Alamos National Laboratory is developing non-precious metal cathode catalysts derived from polyaniline (PANI) [3]. PANI is thick (~100 μm) compared to conventional platinum on carbon (Pt/C) catalysts (0.5 μm to 10 μm). There was a question as to the source of the observed flooding in PANI. To remove the variable of layer thickness, a 50 μm thick Pt/C catalyst was compared to a 75 μm thick PANI catalyst [4]. Figure 1 shows the primary source of transport resistance is PANI is hygroscopic. To obtain higher performance one must either wet-proof PANI or use hydrophilic GDLs on the anode to facilitate water transport out of the PANI.

### Lithium Batteries

Ensuring robust lithium battery operation is critical for these high energy density batteries used in automotive applications. Battery models are used for system control

and rely on estimates of lithium concentration and electrode states. By measuring the lithium concentration directly in an operating battery, neutron imaging can provide unique information to verify model predictions [5]. Several challenges exist for these measurements: very high spatial resolution is required as typical electrodes are 20 μm to 50 μm thick; electrodes tend to be wavy with variations of about ≥10 μm, requiring mechanical flattening or employing tomography; the electrode width of 1 cm to 2 cm can be opaque to neutrons due to the hydrogenous electrolyte. Deuterated electrolytes exist but are expensive and slightly modify battery operation. Although these challenges are difficult at present, they may be met with the development of a neutron microscope.

A recent example of an unsafe lithium battery is the Boeing 787 “Dreamliner” incident [6]. The U.S. National Transportation Safety Board (NTSB) recently completed its investigation of the incident. While the NTSB couldn’t determine the fire’s root cause, they concluded the likely source of the fire was an internal short. NTSB used neutron tomography to look for a lithium salt deposit on the battery header exterior that could have resulted in a short. Figure 2 shows that there was no evidence of such a deposit, supporting the conclusion of an internal short.

## Engineering Materials

### Hydrogen Embrittlement

Hydrogen uptake by steels can result in hydrogen assisted cracking, and numerous pathways exist for hydrogen incorporation into the metal. Researchers at BAM recently demonstrated that neutron tomography could resolve hydrogen blister formation and dissolution in iron with a hydrogen concentration sensitivity of about 5 kmol $m^{-3}$ [7]. This important feasibility study will open the door to further research on embrittlement.

### Strain, Residual Stress, Crystalline Phase

Bragg-edge imaging exploits the increase in transmission when a neutron of a given wavelength can no longer be diffracted by a crystal plane; the change goes as $F_H \lambda^2$ [8]. Pulsed and continuous neutron sources can be efficiently used for Bragg-edge imaging; pulsed sources are preferred to determine an unknown crystal structure; reactor sources are effective for measuring about one crystallographic plane. Recent work used the difference in the crystal structure of martensitic and austenitic steels to map their relative concentrations in deformed samples [9]. The imaging community anticipates Bragg-edge imaging will become a routine method, especially at pulsed sources

### Concrete

Water interacts strongly with concrete during the curing process and can result in severe freeze damage. Controlling water evaporation or ingress is thus critical in determining the concrete service lifetime and many studies employ neutron imaging to reveal water’s role in concrete. One experiment focused on mortars drying effects of shrinkage reducing admixtures (SRAs) [10]. Neutron imaging observed a sharper drying front in the SRA samples, which appears related to increased capillary pressure gradient and higher viscosity.

## Multi-phase Flow

### Heat pipes

Heat pipes (HPs) are efficient, compact cooling devices that remove heat by evaporating a liquid, which is condensed at the cool end. Oscillating HPs are being developed for cooling computers, especially for aerospace applications. Neutron imaging allowed the direct comparison of fluid modeling with observations, leading to insights into the impact of surface wetting properties and inclusion of nanoparticles [11]. Alkali metals, such as lithium, cool in high temperature environments including hypersonic flight. Experiments at NIST (Figure 3) simulated conditions these HPs experience by first induction heating the entire HP to 700 °C and then boost heating with a propane torch to 1250 °C. From these images, effects on lithium flow due to orientation with respect to gravity, presence of non-condensable gases, and wicking structures were observed [12].

### Geology

There are many multiphase flow topics in geological systems that can be addressed with neutron imaging, including geothermal heat transfer [13], phase transformations of rock under temperature and pressure, soil moisture profiles [14], and oil and gas recovery. Neutron imaging enables penetrating a sample environment to image flow patterns in the bulk. As an example, a sandstone rock core, 3.8 cm in diameter, was saturated in oil and placed in a pressure vessel [15]; supercritical $CO_2$ displaced the oil as shown in Figure 4.

### Cryogenic Liquids

While optical ports for cryostats exist, neutrons permit one to use all metallic components. As a demonstration, the phase separation of $^3$He from $^4$He in a dilution refrigerator was imaged; Figure 5 shows the sample above and below the phase separation temperature [16]. NASA is developing cryogenic propellant storage tanks for operation in microgravity environments; measuring the contact angle of the cryogens during evaporation and condensation is essential. The first demonstration experiments observed a 10° contact angle between liquid hydrogen and aluminum and future experiments varying container and propellant are planned [17].

## Future capabilities and measurement goals

While the development of new contrast mechanisms provides many new research opportunities, in our view there are three essential improvements for neutron imaging to further its range of applications: higher spatial resolution (≤1 μm); increased time resolution (×10 to ×100); strain measurements with ~10 με resolution.

One avenue to 1 μm spatial resolution is to improve imaging detectors. Recent work on the neutron macroscope shows good promise for resolution of a few microns [18]. Using Timepix detectors, it was shown that it is possible to measure ionizing particle paths from a LiF converter to reach resolution of a few micrometers [19]. Work on intagliated scintillators for neutron imaging can achieve a resolution of about 5 μm [20].

While improvements in the intrinsic spatial resolution of detectors are important efforts, they do not address time resolution. Image acquisition time is related to neutron flux. Traditional neutron imaging uses pinhole optics geometry; to have acceptable geometric blur one must collimate the beam. For imaging with 10 μm resolution the typical neutron flux is ~$10^6$ $cm^{-2}$ $s^{-1}$; the count of a 1 μm pixel is 0.01 $s^{-1}$. By using a reflective neutron lens which requires no collimation one can: increase the time resolution and ×100 is feasible; use neutron image magnification to improve the resolution of the detector, with 10x being feasible to reach 1 μm; such “Wolter optics” are under development [21].

Metallic additive manufacturing (MAM) has many tunable parameters that impact the residual stress of the part. Being able to measure the stress in buried features would greatly speed the development of MAM. Neutron imaging could provide these measurements, but one must improve the strain measurements to better than 100 με (ideally 10 με). As well, work is required to determine under what conditions it will be possible to convert the scalar tomography measurements into tensorial strain components [22].

## Conclusions

Neutron imaging is a valuable tool for many industrial and basic research fields. There is a continuous effort in the neutron imaging community to develop or adapt new image contrasts to gain deeper insight into materials. We believe that these efforts within five years will realize image spatial resolution of better than 1 μm with time resolution of the order 100 s.

## Acknowledgments

The authors thank Dr. K. Kihm, University of Tennessee, for photo permission in Figure 3; Mr. D. O’Kelley (NIST) produced Figure 4 as a NIST SURF project; Dr. P. Guman, University of Waterloo, for images in Figure 5.

### Funding

This work was supported by the U.S. Department of Commerce, the NIST Radiation Physics Division, the Director’s office of NIST, the NIST Center for Neutron Research, and the Department of Energy interagency agreement No. DE_AI01-01EE50660.

## References

1. Trabold TA, Owejan JP, Gagliardo JJ, Jacobson DL, Hussey DS, Arif M, “Use of neutron imaging for proton exchange membrane fuel cell (PEMFC) performance analysis and design”, in: Handbook of Fuel Cells – Fundamentals, Technology and Applications. Eds. Vielstich W, Yokokawa H, Gasteiger HA. Volume 6: Advances in Electocatalysis, Materials, Diagnostics and Durability. John Wiley & Sons (2009).
2. Arif M, Jacobson DL and Hussey DS, “Neutron Imaging Study of the Water Transport in Operating Fuel Cells”, pp. 686–692, DOE Hydrogen Program FY 2010 Annual Progress Report, 2010.
3. Wu G, More KL, Johnston CM and Zelenay P, Science 332, 443 (2011). [PubMed: 21512028]
4. Hussey DS, Spernjak D, Wu G, Jacobson DL, Liu D, Khaykovich B, Gubarev MV, Fairweather J, Mukundan R, Lujan R, Zelenay P, and Borup RL, “Neutron Imaging Of Water Transport In Polymer-Electrolyte Membranes And Membrane-Electrode Assemblies”, ECS Transactions 58(1), 293–299 (2013).

5. Siegel JB, Lin X, Stefanopoulou AG, Hussey DS, Jacobson DL, and Gorsich D, Neutron Imaging of Lithium Concentration in LFP Pouch Cell Battery. Journal of the Electrochemical Society 158, A523–A529 (2011).
6. National Transportation Safety Board (NTSB) Aircraft Incident Report, "Auxiliary Power Unit Battery Fire Japan Airlines Boeing 787–8, JA829J Boston, Massachusetts January 7 2013", http://www.ntsb.gov/investigations/AccidentReports/Reports/AIR1401.pdf
7. Griesche A, Dabah E, Kannengiesser T, Kardjilov N. Hilger A, Manke I, "Three-dimensional imaging of hydrogen blister in iron with neutron tomography", Acta Materialia 78, 14–22 (2014).
8. Vogel S, Bourke MAM, Hanan JC, Priesmeyer H-G, Uestuendag E, "Non-destructive in-situ real-time measurements of structural phase transitions using neutron transmission", Advances in X-ray Analysis 44, 75–84 (2001).
9. Woracek R, Penumadu D, Kardjilov N, Hilger A, Boin M, Banhart J, and Manke I, "3D Mapping of Crystallographic Phase Distribution using Energy-Selective Neutron Tomography", Adv. Mater 26, 4069–4073 (2014). [PubMed: 24692200]
10. Villani C, Lucero C, Bentz D, Hussey D, Jacobson DL and Weiss WJ, "Neutron Radiography Evaluation of Drying in Mortars with and without Shrinkage Reducing Admixtures", American Concrete Institute Fall Meeting, Washington, D.C. 26 OCT 2014.
11. Yoon I, Wilson C, Borgmeyer B, Winholtz RA, Ma HB, Jacobson DL, Hussey DS, "Neutron phase volumetry and temperature observations in an oscillating heat pipe", International Journal of Thermal Sciences 60, 52–60 (2012).
12. Kihm KD, et al., J. Heat Transfer, 136(8), 080903 (2014).
13. Polsky Y, et al. Particle Imaging Velocimetry Technique Development for Laboratory Measurement of Fracture Flow Inside a Pressure Vessel Using Neutron Imaging, Proceedings, Fortieth Workshop on Geothermal Reservoir Engineering, Stanford University, Stanford, California, January 26–28, 2015, SGP-TR-204.
14. Cheng CL, Kang M, Perfect E, Voisin S, Horita J, Bilheux HZ, Warren JM, Jacobson DL, and Hussey DS, Average soil water retention curves measured by neutron radiography, Soil Science Society of America Journal 76(4), 1184–1191 (2012).
15. Polsky Y, Anovitz LM, Bingham P, Carmichael C, Application of Neutron Imaging to Investigate Flow Through Fractures for EGS, Proceedings, 38th Workshop on Geothermal Reservoir Engineering, Stanford University, Stanford, CA, February 11–13, 2013.
16. Gumann P, Scherschligt J, Hussey D, Jacobson D, Cory D, Taminiau I, 3He-4He liquid mixtures investigated by neutron imaging technique at low temperatures, American Physical Society, APS March Meeting 2012, February 27–March 2, 2012, abstract #S1.310.
17. Bellur K, Medici E, Allen J, C-K Choi J Hermanson, Tamilarasan A, Hussey D, Jacobson D, Leo J, and McQuillen J, Neutron Radiography of Condensation and Evaporation of Hydrogen in a Cryogenic Condition, accepted, Journal of Heat Transfer (2015).
18. Williams SH, Hilger A, Kardjilov N, Manke I, Strobl M, Douissard PA, Martin T, Riesemeier H and Banhart J, Detection system for microimaging with neutrons, Journal of Instrumentation 7, P02014 (2012).
19. Vavrik D, Holik M, Jakubek J, Jakubek M, Kraus V, Soukup P, Turecek D, Vacik J, Modular pixelated detector system for neutron imaging with micrometric resolution, Proceedings, World Conference on Neutron Radiography, Grindelwald, Switzerland, October 5–10, 2014.
20. Trtik P, Hovind J, Gruenzweig C, Bollhalder A, Thominet V, David C, Kaestner A, Vontobel P, and Lehmann EH, Extending the spatial resolution of neutron imaging facilities at PSI – The neutron microscope project, Proceedings, World Conference on Neutron Radiography, Grindelwald, Switzerland, October 5–10, 2014.
21. Liu D, Hussey D, Gubarev MV, Ramsey BD, Jacobson D, Arif M, Moncton DE, and Khaykovich B, Demonstration of Achromatic Cold-Neutron Microscope Utilizing Axisymmetric Focusing Mirrors, Applied Physics Letters 102, 183508 (2013).
22. Abbey B, Zhang SY, Vorster W, Korsunsky AM, Reconstruction of axisymmetric strain distributions via neutron strain tomography, Nuclear Instruments and Methods in Physics Research B, 270 (2012) 28–35; H. Sato et al., Development of the tensor CT algorithm for strain

tomography using Bragg-edge neutron transmission, Proceedings, World Conference on Neutron Radiography, Grindelwald, Switzerland, October 5–10, 2014.

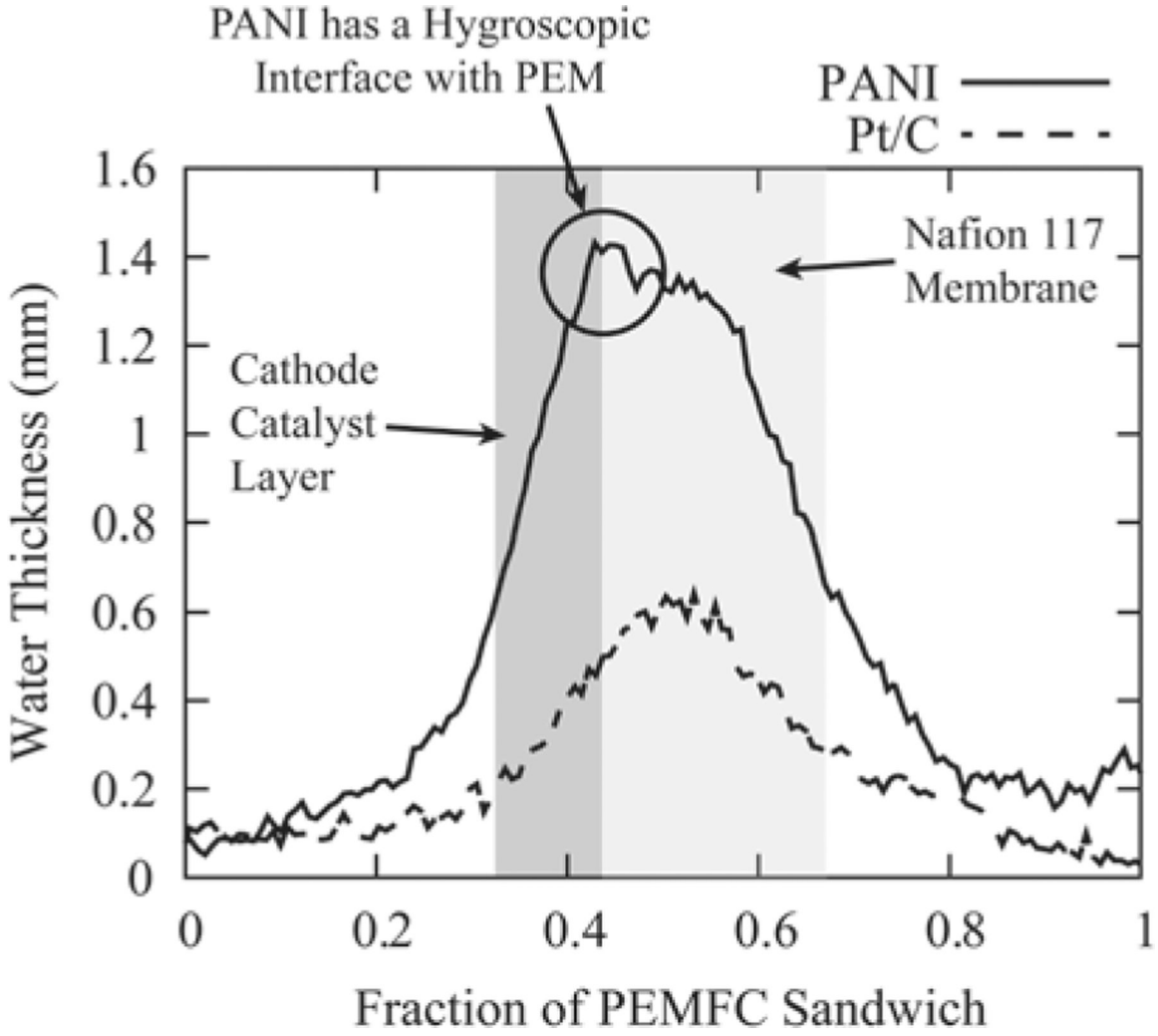


**Figure 1.**
Comparison of a PEMFC with a PANI catalyst and thick Pt/C catalyst at 50 % relative humidity and open circuit voltage.

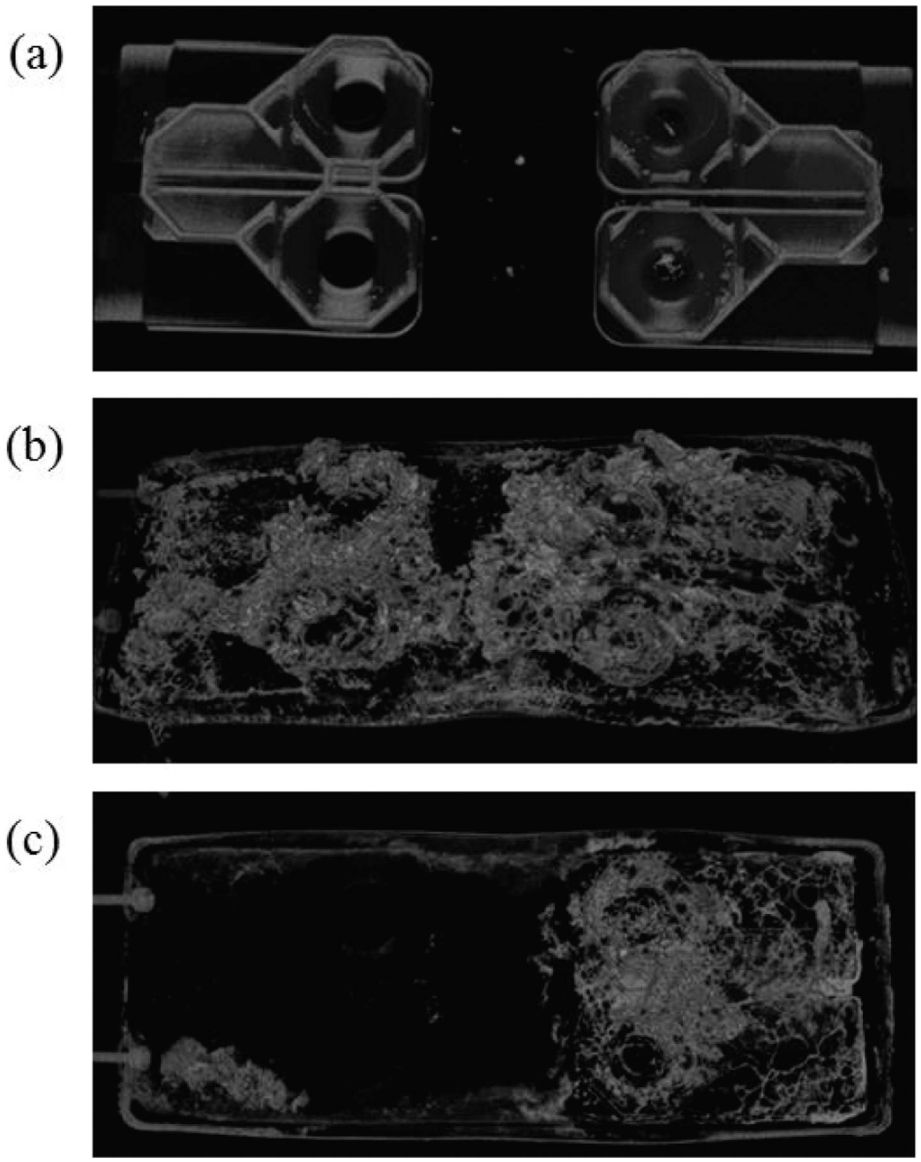


**Figure 2.**
Neutron attenuation of battery headers from the Dreamliner fire, (a) cell 2 (b) cell 5 (c) cell 6; cells 5 and 6 were the cells in which the fire started, cell 2 suffered minimal damage.

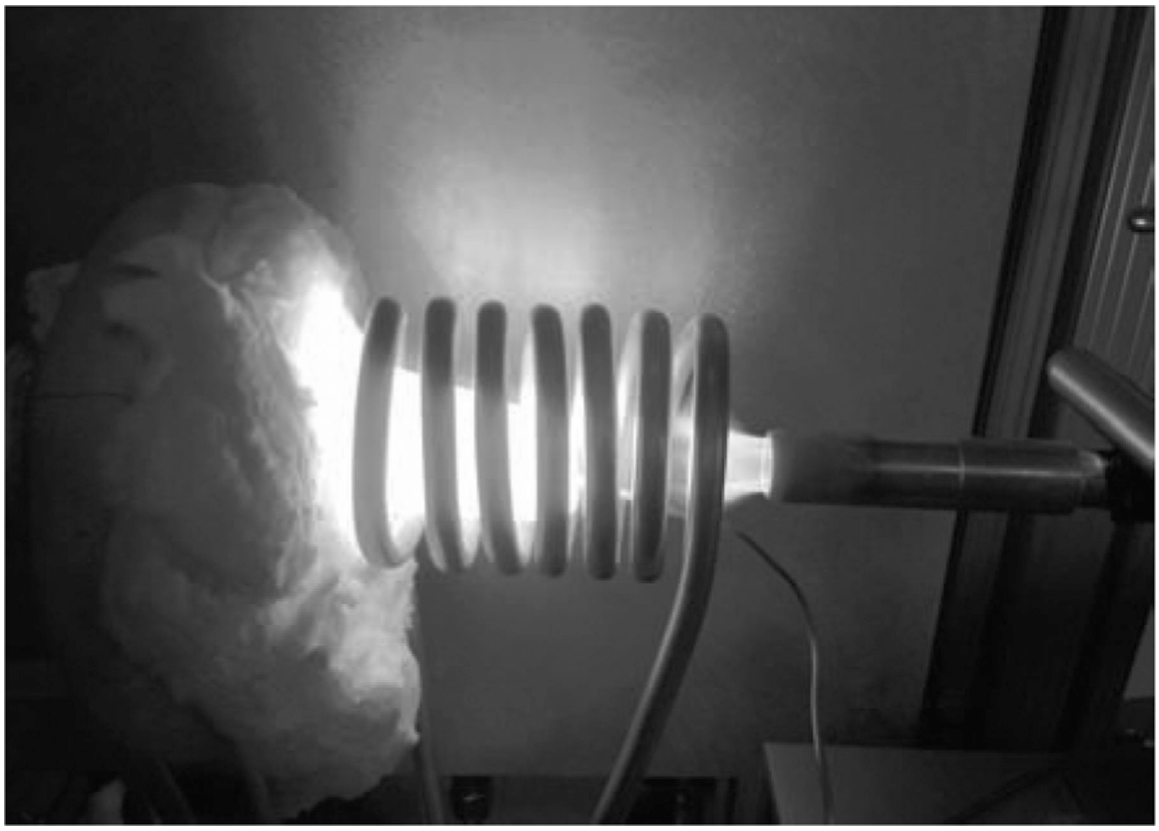

**Figure 3.**
Experimental setup of a lithium HP at NIST. (Photo courtesy of Dr. K. Kihm, University of Tennessee.)

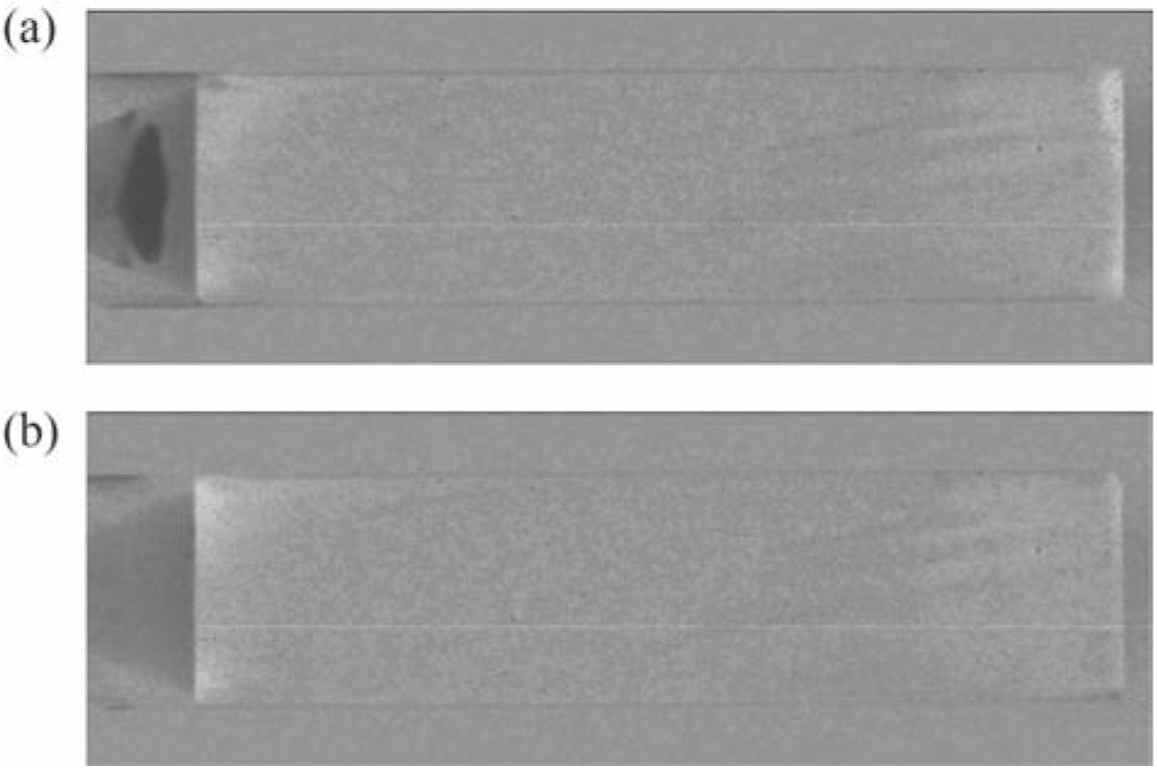


**Figure 4.**

Two images during supercritical $CO_2$ extraction of oil from a sandstone core. Dark regions contain removed oil or $CO_2$, ligher regions correspond to removal of oil. (Photo courtesy of Mr. D. O'Kelley, NIST.)

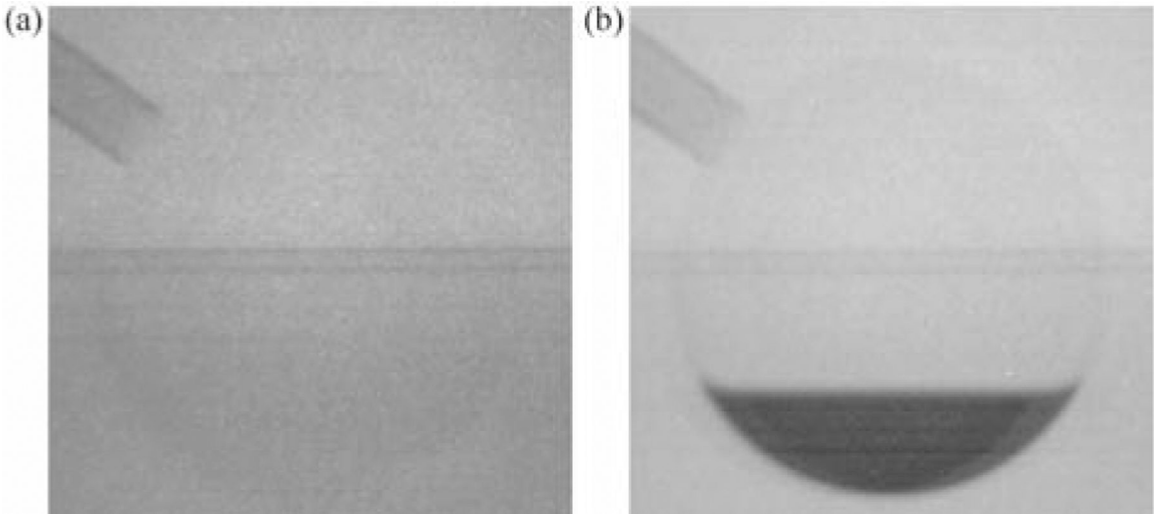


**Figure 5.**
Phase separation of $^{3}$He from $^{4}$He, (a) mixture before, (b) and after phase separation, the region of $^{3}$He is darker than $^{4}$He. (Photo courtesy of Dr. P.Guman, University of Waterloo.)